Positron emission tomography (PET) is a powerful noninvasive molecular imaging technique that provides high sensitivity, good spatial resolution, and easy and accurate quantification; PET is frequently used in biological research and clinical studies.[3] Radionuclides used in PET include short-lived radioisotopes (^{11}C, ^{13}N, ^{15}O) of the abundant elements in the structures of biologically active compounds, such as natural products and drugs, etc. A dose of the labeled compound in medicine is very tiny, namely less than 1/100 of actual pharmacological dose or 100 μg.[4] Therefore, the application of PET in a human microdose study at an early stage of drug and biomarker development has been expected.[5] The increasing need for pharmacologically significant PET tracers requires efficient synthetic strategies for new molecular tracer designs and advances in radiolabeling methodology. Carbon-11 (half-life = 20.4 min) is one of the most important isotopes for PET research. In particular, the incorporation of the [^{11}C]methyl group into organic frameworks through [^{11}C]carbon–carbon bond formation is one of the attractive approaches because 1) the [^{11}C]methyl group can be introduced into a metabolically stable position in the molecules and, therefore, such a ^{11}C-labeled tracer provides a highly credible PET image, 2) the methyl group is often used in drug design to control the lipophilicity of the molecule and the blocking of the metabolic position as the smallest substituted group containing carbon, and 3) the short half-life of the ^{11}C-incorporated tracer allows rapid screening of the PET images and increases progress by several trials per day.[6]

Since the discovery of COX-2, the development of drugs that selectively inhibit this isoform and the development of corresponding specific PET tracers have become a major area of pharmaceutical research.[7] During the past decade, PET tracers corresponding to highly selective and potent COX-2 inhibitors, such as [^{18}F]desbromo-Dup-697,[8] [^{11}C]Celecoxib,[9] [^{11}C]Rofecoxib,[10] and [^{11}C]Valdecoxib[11] have been developed. Additionally, ^{11}C-labeling of diaryl-substituted imidazole and indole analogues has yielded PET probes with a high affinity and selectivity for COX-2.[12] However, to the best of our knowledge, the successful COX-2 imaging by using these PET tracers has not yet been reported.[13]

The cause of the adverse side effects of NSAIDs is suspected to be the inhibition of COX-1, a necessary housekeeping gene that is not elevated during inflammation. In contrast, COX-2 is normally nondetectable in most tissues, but is rapidly elevated during inflammation. Thus, the inhibition of COX-2 by NSAIDs is thought to be responsible for their therapeutic effects. However, the relative biological contributions of COX-1 and COX-2 isoforms in the maintenance of normal physiological functions and in disease states are not entirely clear.[14] Therefore, the development of both nonselective and selective COX inhibitors and the evaluation of their in vivo behavior by PET imaging could greatly help to elucidate their physiological actions.

We previously developed a simple method to synthesize [^{11}C]Celecoxib, a COX-2 inhibitor.[15] In the present report, we describe the efficient general syntheses of ^{11}C-labeled 2-arylpropionic esters by rapid [^{11}C]methylation through sp^3–sp^3-type coupling by the reaction of [^{11}C]CH_3I and the corresponding enolates with the aim of realizing COX imaging by PET. These esters were readily converted to the corresponding acids as NSAID structures by one-pot hydrolysis.[16] The evaluation of the blood-brain barrier (BBB) permeability of these NSAIDs PET tracers in rats and in vivo studies of a rat lipopolysaccharide (LPS)-induced inflammation model are also described.

Results and Discussions

Chemistry: The 2-arylpropionic acids of six NSAIDs, Ibuprofen, Naproxen, Flurbiprofen, Fenoprofen, Ketoprofen, and Loxoprofen, were selected for ^{11}C-labeling. They share a common chemical structure for [^{11}C]methyl group introduction, despite their different levels of inhibition of COX-1 and COX-2.[17] All precursors and authentic samples were prepared according to conventional synthetic methods or purchased as described in the Experimental Section.[18]

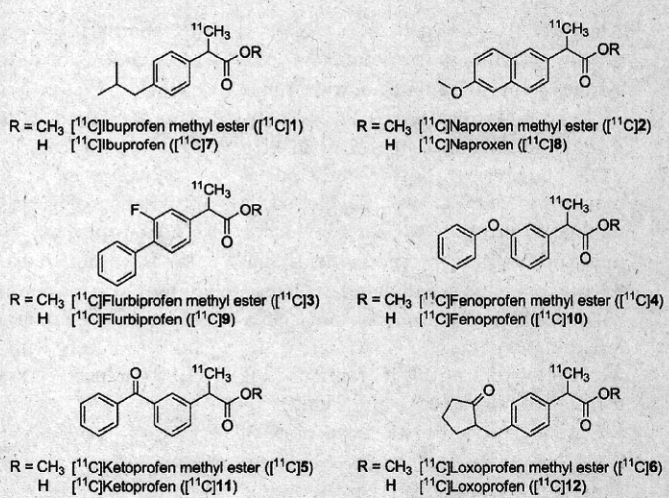

Radiochemistry: Scheme 1 illustrates the syntheses of ^{11}C-labeled 2-arylpropionic acids and their esters; the syntheses were based on rapid *C*-[^{11}C]methylation by using [^{11}C]CH_3I under basic conditions. In general, sodium hydride was added to a solution of methyl arylacetate as a precursor in

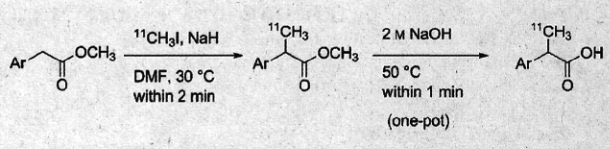

Scheme 1. Syntheses of ^{11}C-labeled 2-arylpropionic acids and their methyl esters.

DMF at room temperature for the deprotonation of the benzylic position. After 10–20 min, [^{11}C]CH_3I with He flow (30 mL min^{-1}) was trapped in the mixture and reacted with the enolate at 30 °C for 2 min, and then the resulting mixture was quickly subjected to the preparative HPLC operation because of the rapid completion of the *C*-[^{11}C]methylation. When the reaction was continued for a slightly longer time or at a slightly higher temperature after [^{11}C]CH_3I trapping, the yield of the [^{11}C]methylated compounds was decreased. In the synthesis of [^{11}C]Ketoprofen methyl ester ([^{11}C]**5**), when the reaction mixture was heated at 50 °C or left for several minutes after [^{11}C]CH_3I trapping, the desired product [^{11}C]**5** was gradually decomposed with time, and some unknown side products appeared (Figure 1).

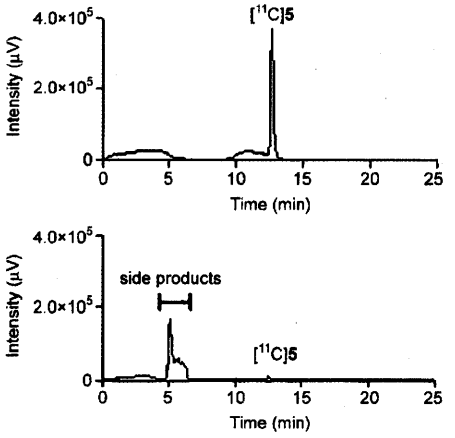

Figure 1. Radiochromatograms of the crude reaction mixture of [^{11}C]Ketoprofen methyl ester ([^{11}C]**5**) obtained by the reaction of [^{11}C]CH_3I and methyl (3-benzoylphenyl)acetate, demethylated precursor. A) [^{11}C]CH_3I trapping at 30 °C for 2 min. B) [^{11}C]CH_3I trapping at 30 °C for 2 min and reaction at 50 °C for 4 min.

Finally, [^{11}C]**5** was almost completely decomposed after the reaction for 4 min at 50 °C (Figure 1B). After extensive experiments, we found that the reaction was completed during [^{11}C]CH_3I trapping at 30 °C without further reaction time. This reaction was also proceeded by [^{11}C]CH_3I trapping at −10 °C. By using these conditions, [^{11}C]Ibuprofen methyl ester ([^{11}C]**1**), [^{11}C]Naproxen methyl ester ([^{11}C]**2**), [^{11}C]Flurbiprofen methyl ester ([^{11}C]**3**), [^{11}C]Fenoprofen methyl ester ([^{11}C]**4**), and [^{11}C]Loxoprofen methyl ester ([^{11}C]**6**) were efficiently synthesized. Inexplicably, the compounds, [^{11}C]**1**, [^{11}C]**2**, [^{11}C]**5**, and [^{11}C]**6** tended to decompose upon radiolyses. In particular, [^{11}C]**1** and [^{11}C]**2** were gradually decomposed during HPLC purification or concentration by evaporator. However, in our experience, we have found that such radiolyses could be prevented by the use of [^{11}C]CH_3I at less than 15 GBq. The addition of ascorbic acid as an antioxidant stabilizer to the reaction mixture before the HPLC purification also effectively prevented the radiolysis.[19] Consequently, we found that the six kinds of 2-aryl-[^{11}C]propionic acid methyl esters are stable for 2 h after purification by analytical HPLC. At present, the mechanism of the radiolytic decomposition and the intrinsic stability of the methyl esters are not clear. In addition, the corresponding carboxylic acids, [^{11}C]Ibuprofen ([^{11}C]**7**), [^{11}C]Naproxen ([^{11}C]**8**), [^{11}C]Flurbiprofen ([^{11}C]**9**), [^{11}C]Fenoprofen ([^{11}C]**10**), [^{11}C]Ketoprofen ([^{11}C]**11**), and [^{11}C]Loxoprofen ([^{11}C]**12**), were also synthesized in one-pot reactions by the rapid hydrolysis of each 2-aryl[^{11}C]propionic acid methyl ester with 2 M sodium hydroxide at 50 °C for 1 min. This hydrolysis completed even at 30 °C for 1 min. Interestingly, ^{11}C-labeled 2-arylpropionic acids were radiochemically stable. The physicochemical properties of the labeled compounds are listed in Table 1. All 12 ^{11}C-labeled compounds

Table 1. Synthetic results and the stability of ^{11}C-labeled 2-arylopropionic acids and their methyl esters.

Compound	Radioactivity [GBq][a]	Specific radioactivity [GBq μmol^{-1}]	DCY [%]	Stability[b]
methyl ester				
[^{11}C]**1**	3.1±0.8	20±2.9	56±17	C
[^{11}C]**2**	2.4±0.1	32±7.6	48±5.7	C
[^{11}C]**3**	5.5±0.2	40±1.5	76±12	A
[^{11}C]**4**	2.9±1.9	38±5.6	43±24	A
[^{11}C]**5**	5.5±0.4	47±11	72±13	B
[^{11}C]**6**	1.9±0.1	26±8.7	26±5.3	B
carboxylic acid				
[^{11}C]**7**	4.3±0.7	25±8.5	72±15	A
[^{11}C]**8**	2.7±0.6	24±1.0	47±12	A
[^{11}C]**9**	2.8±0.3	31±12	43±6.7	A
[^{11}C]**10**	3.3±2.3	20±5.0	60±21	A
[^{11}C]**11**	3.0±0.6	30±15	29±13	A
[^{11}C]**12**	1.6±0.6	22±6.9	29±13	A

Data are expressed as mean ±SD ([^{11}C]**1**, [^{11}C]**2**, [^{11}C]**3**, [^{11}C]**4**, [^{11}C]**7**, [^{11}C]**9**, [^{11}C]**10**, [^{11}C]**11**, and [^{11}C]**12**, $n=3$; [^{11}C]**5**, [^{11}C]**6**, and [^{11}C]**8**, $n=4$). [a] Radioactivity showing the isolated radioactivity. [b] A: stable, B: stable in the presence of ascorbic acid, C: stable under the lower current beam and in the presence of ascorbic acid; DCY: decay-corrected yield based on [^{11}C]CH_3I.

that we synthesized by the above procedures possessed sufficient radioactivity (1.7–5.5 GBq) for an animal PET study. The decay-corrected radiochemical yields (DCY) based on [^{11}C]CH_3I were 26–76%. Of these, the yields of [^{11}C]**12** and its methyl ester [^{11}C]**6** were relatively low. Such low yields were presumably due to the co-occurrence of the enolization at both of the α-positions of the ester and ketone moieties. We classified isolated [^{11}C] products into three groups based on their radiochemical stability. [^{11}C]**3**, [^{11}C]**4**, [^{11}C]**7**, [^{11}C]**8**, [^{11}C]**9**, [^{11}C]**10**, [^{11}C]**11**, and [^{11}C]**12** were stably isolated without the addition of ascorbic acid, and they were categorized as class A. [^{11}C]**5** and [^{11}C]**6** in class B required ascorbic acid for the HPLC purification and evaporation. [^{11}C]**1** and [^{11}C]**2** in class C were very unstable, and they required not only ascorbic acid but also synthetic conditions with the lower radioactivity (~15 GBq). The reaction with higher radioactivity (>15 GBq) gave many kinds of products among which it was too difficult to isolate the desired labeled compound. The chemical and radiochemical purities of the isolated products were greater than 98% because of their un-

expectedly ready separation from their corresponding demethylated precursors.[20] Here, we consider that such a large polarity difference between methylated and demethylated compounds, as indicated in reverse-phase HPLC, may be caused by the following electronic and structural factors: The first factor is the ordinary increase of hydrophobicity by introducing a nonpolar methyl group into an organic framework. The second factor is the decrease of the acidity of the benzylic proton of methylated compounds that is attributed to the hyperconjugation between the C–H σ bond of a benzylic position and C=O π*, which is also possible for the LUMO (π*) of a phenyl moiety. Such hyperconjugation in methylated products, if any, would also be less favored in the methylated compound because of steric congestion emerging from the assumed fully substituted pseudo olefin structure.

Brain penetration of [^{11}C]5 and [^{11}C]11 evaluated by microPET imaging: PET scans were performed to measure the uptake of [^{11}C]**5** and [^{11}C]**11** in the inflamed area of the left striatum in rats; the inflammation was induced by the injection of 50 μg of lipopolysaccharide (LPS) one day before the PET scan, because it was reported to cause the activation of microglia within 24 h.[21] In this condition, we have also observed the increase of the COX-2 expression surrounding the LPS injection site by the immunohistochemical method (data not shown). Radioactivity of [^{11}C]**5** after intravenous bolus administration was highly accumulated into the LPS injection site and the surrounding area, whereas radioactivity of [^{11}C]**11** after the administration was not accumulated in the brain including the injected site (Figure 2). The radioactivity of [^{11}C]**5** in the inflammatory area was about 9-fold higher than that of [^{11}C]**11**. Low penetration of [^{11}C]**11** into the brain, which was consistent with a previous study that used 2-arylpropionic acids,[22] was dramatically improved by the conversion of carboxylic acid into methyl ester.[23] As compared with [^{11}C]PK11195, which is one of the PET tracers widely used for the imaging of activated microglia that have occurred by neuroinflammation, the SUV level of [^{11}C]**5** in the brain is almost the same, and moreover, the ratio of radioactivity in the inflammatory region to background is rather superior.[24] Therefore, [^{11}C]**5** could be applicable for the PET imaging of neuroinflammation.

Measurement of [^{11}C]5 and the radioactive metabolites in rat brain and blood: Metabolite analyses in rat brain and blood of the ester as proradiotracers were performed in normal rats after the administration of [^{11}C]**5** (Figure 3). [^{11}C]**5** was rapidly hydrolyzed in rat blood to the pharmacologically active form [^{11}C]**11**, and the hydrolysis rate of [^{11}C]**5** in rat brain was much slower than that in the blood. Thus more than 90% of [^{11}C]**5** that passed the BBB was hydrolyzed to [^{11}C]**11** within 5 min after administration. Though the first hydrolysis step should be considered for the quantitative kinetic analysis of PET, the hydrolysis rate of [^{11}C]**5** might be fast enough for the functional analysis of COX imaging in rat brain, because a significant difference between the inflammatory region and contralateral region was observed in the later time point after the injection (Figure 2B). Thus, [^{11}C]**5** showed appropriate behavior as a proradiotracer for the functional imaging in the rat brain.

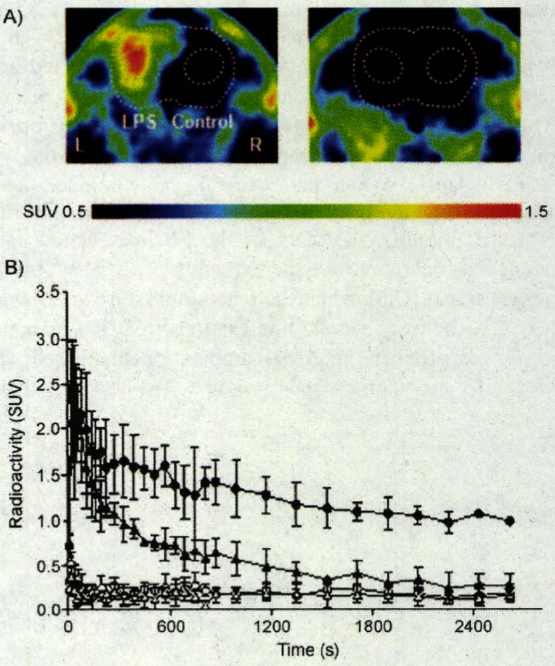

Figure 2. A) Summated PET images (from 5 to 45 min after the tracer injection) of [^{11}C]**5** (left panel) and [^{11}C]**11** (right panel) in rat brain inflammation induced by LPS (50 μg) injection into the left striatum. B) Time–activity curves of [^{11}C]**5** ($n=2$) and [^{11}C]**11** ($n=3$) in the LPS-injected inflammatory area (LPS) and the contralateral region (control). Data are expressed as mean ±SD (●: LPS [^{11}C]**5**, ▲: control [^{11}C]**5**; ○: LPS [^{11}C]**11**, △: control [^{11}C]**11**).

Screening study of 2-aryl[^{11}C]propionic acid methyl esters by microPET imaging: To explore the appropriate PET tracers for neuroinflammation, PET studies by using [^{11}C]**1**, [^{11}C]**2**, [^{11}C]**3**, [^{11}C]**4**, [^{11}C]**5**, and [^{11}C]**6** were performed in the rat model of neuroinflammation. PET images with 2-aryl[^{11}C]propionic acid methyl esters demonstrated that all of the proradiotracers, with the exception of [^{11}C]**1**, showed high accumulation in the area of LPS-induced inflammation (Figure 4). Since the radiochemical stability of [^{11}C]**1** was comparable with that of [^{11}C]**2**, the lower brain uptake of [^{11}C]**1** might be derived from the differences of pharmacokinetic properties, such as metabolic stability and/or affinity for efflux pumps at the BBB. Regional brain accumulation of these proradiotracers is shown as a standardized uptake value (SUV) during 40 min (5–45 min post-injection of the tracer) in Table 2. The highest accumulation in the inflammatory area was observed for [^{11}C]**5**, followed by [^{11}C]**6**, [^{11}C]**3**, [^{11}C]**4**, and [^{11}C]**2**, whereas the ratio to the contralateral lesioned area was the highest for [^{11}C]**6** and [^{11}C]**2** (about 4-fold).

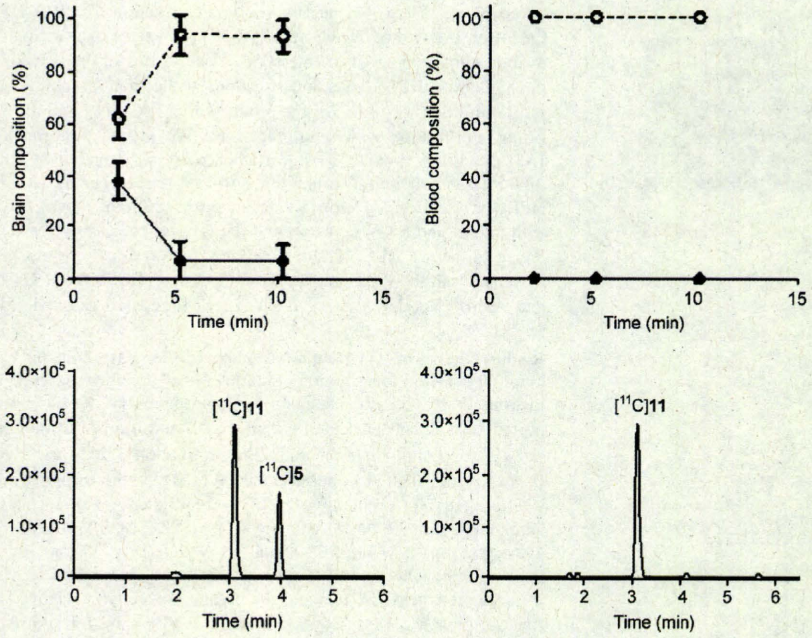

Figure 3. Rat brain (left) and blood (right) compositions of Ketoprofen methyl ester ([^{11}C]**5**, ●) and its pharmacological active metabolite, Ketoprofen ([^{11}C]**11**, ○). Data are expressed as mean ±SD (n=3). Top) Composition of [^{11}C]**5** and [^{11}C]**11**. Bottom) HPLC analyses by radio detector after 2 min.

the ex vivo autoradiography study also revealed the significant reduction of increased radioactivities in the LPS-injected side of the striatum and cortex (Figure 5C). Since many inflammatory-related events, such as organ infiltration and invasion of immune cells, are known to hardly occur in the early phase of inflammation, the incomplete blocking result observed in the inflammatory area may be derived from large amounts of nonspecific accumulation caused by such events.

Currently, PET and related biological studies are being conducted with rodents and nonhuman primates to determine the suitable NSAID PET tracers for in vivo COXs imaging, which is useful for diagnosis and drug development for diseases relating to COXs expression.

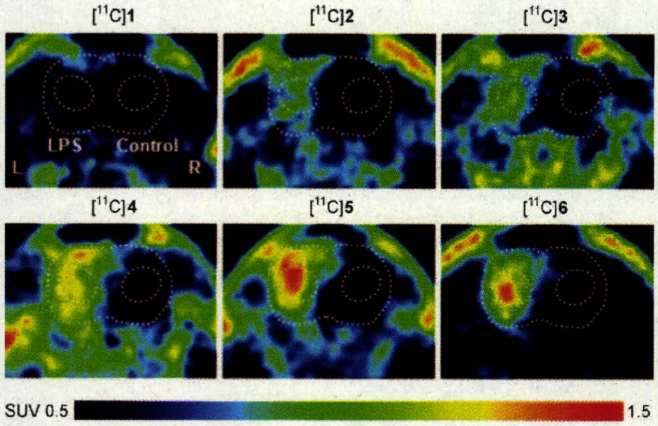

Figure 4. PET images of 2-aryl[^{11}C]propionic acid methyl esters in rat brain inflammation induced by LPS (50 μg) injection into the left striatum.

Table 2. Regional brain accumulation of the 2-aryl[^{11}C]propionic acid methyl esters in the inflammatory area induced by LPS (50 μg) injection into the left striatum.[a]

	SUV LPS injected striatum	contralateral striatum	Ratio LPS/control
[^{11}C]**1**	0.51±0.07	0.30±0.04	1.70±0.24
[^{11}C]**2**	0.92±0.17	0.26±0.02	3.57±0.70
[^{11}C]**3**	0.96±0.03	0.39±0.03	2.50±0.27
[^{11}C]**4**	0.93±0.17	0.39±0.16	2.57±0.63
[^{11}C]**5**	1.21±0.18	0.47±0.12	2.75±1.10
[^{11}C]**6**	1.10±0.18	0.29±0.02	3.76±0.48

[a] The data were expressed as the standardized uptake value (SUV), normalized for injected radioactivity and body weight. SUV=(radioactivity per cubic centimeter tissue/injected radioactivity)×gram body weight. Data are expressed as mean ±SD ([^{11}C]**3** and [^{11}C]**5**, n=2; [^{11}C]**1**, [^{11}C]**2**, [^{11}C]**4**, and [^{11}C]**6**, n=3).

To determine the binding specificity of 2-aryl-[^{11}C]propionic acid methyl esters as proradiotracer in the inflamed area, we performed blocking experiments of [^{11}C]**5** (proradiotracer of [^{11}C]**11**) by using PET and ex vivo autoradiography. Simultaneous injection of authentic Ketoprofen methyl ester (KTP-Me) (10 mg kg^{-1}) with [^{11}C]**5** resulted in a significantly reduced accumulation of radioactivities in the area of LPS-induced inflammation (Figure 5A,B). Images of [^{11}C]**5** (proradiotracer of [^{11}C]**11**) at 50 min post-injection in

Conclusion

To construct a PET tracer library, we developed a method for common and efficient rapid ^{11}C-labeling of 2-arylpropionic acids and their methyl esters through the [^{11}C]carbon–carbon bond formation; this method provided a moderate radiochemical yield with high chemical and radiochemical purity.[25] Although the pharmacologically active forms, 2-aryl[^{11}C]propionic acids, showed low levels of brain uptake, we expect that these compounds will be applied to peripheral imaging. On the other hand, 2-aryl[^{11}C]propionic acid methyl esters showed good brain penetration. In addi-

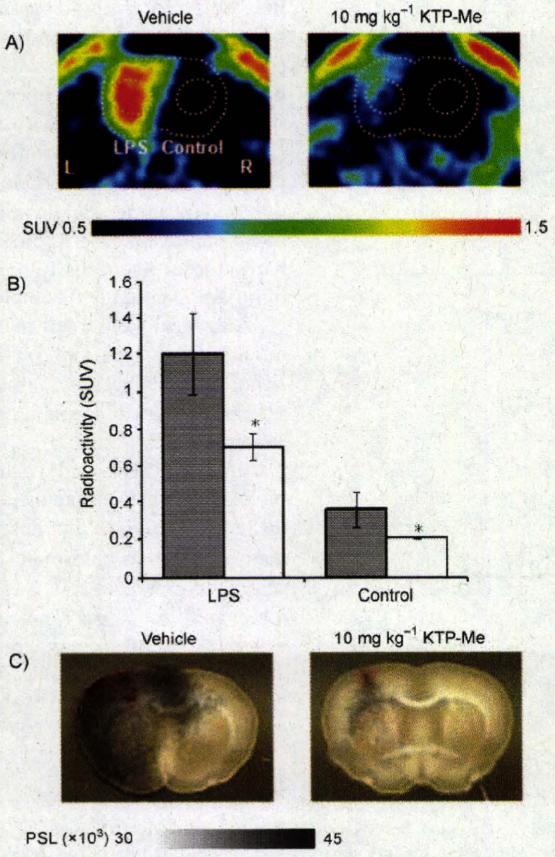

Figure 5. A) PET images of [^{11}C]**5** blocked by excess unlabeled Ketoprofen methyl ester (KTP-Me) in rat brain inflammation induced by LPS (0.5 μg) injection into the left striatum. Unlabeled KTP-Me (10 mg kg^{-1}) was simultaneously administered with radiotracer. B) Accumulated radioactivity of [^{11}C]**5** with simultaneous injection of KTP-Me in the inflamed area (LPS) and the contralateral region (control). The data are expressed as SUV. The results are means ± SD (Vehicle (■), $n=5$; 10 mg KTP-Me (□), $n=4$). *: $p<0.05$; unpaired t-test. C) Ex vivo autoradiographic images of [^{11}C]**5** at 50 min post-injection. The autoradiographic images coregistered with their brain-slice photographs.

tion, the metabolite analysis of the ester [^{11}C]**5** in the rat brain showed that it was converted into the pharmacologically active form [^{11}C]**11**. The studies of a rat model of LPS-induced brain inflammation showed that [^{11}C]**2**, [^{11}C]**3**, [^{11}C]**4**, [^{11}C]**5**, and [^{11}C]**6** were more highly taken up into the LPS-treated area than the contralateral nontreated area. The blocking study in PET and ex vivo autoradiography revealed the specificity of [^{11}C]**5** (proradiotracer of [^{11}C]**11**) for the target regions.

Experimental Section

Chemistry: All chemicals and solvents were purchased from Sigma–Aldrich Japan (Tokyo, Japan), Wako Pure Chemical Industries (Osaka, Japan), Tokyo Kasei Kogyo (Tokyo, Japan), and Nacalai Tesque (Kyoto, Japan), and were used without further purification. Carbon-11 was produced by an ^{14}N(p,α)^{11}C nuclear reaction by using a CYPRIS HM-12S Cyclotron (Sumitomo Heavy Industry, Tokyo, Japan). An original automated radiolabeling system consisting of the heating of the reaction mixture, dilution, HPLC injection, fractional collection, evaporation, and sterile filtration was used for the production of [^{11}C]CH_3I and the ^{11}C-labeling. Purification with semi-preparative HPLC was performed on a JASCO system (Tokyo, Japan). Radioactivity was quantified with an ATOMLAB^{TM}300 dose calibrator (Aloka, Tokyo, Japan). Analytical HPLC was performed on a Shimadzu system (Kyoto, Japan) equipped with pumps and a UV detector, and the effluent radioactivity was determined by using a RLC700 radio analyzer (Aloka). The columns used for the analytical and semi-preparative HPLC were COSMOSIL $5C_{18}$ MS-II and AR-II (Nacalai Tesque). [^{11}C]CH_3I was prepared as previously described.[26]

Radiosynthesis of [^{11}C]Ibuprofen methyl ester (1): Sodium hydride (1 mg) was added to a solution of methyl (4-isobutylphenyl)acetate in anhydrous DMF (200 μL) under an Ar atmosphere. [^{11}C]CH_3I was transported by a stream of helium (30 mL min^{-1}) and trapped in the mixture at 30 °C for 2 min. After the addition of a solution of 25% ascorbic acid (50 μL), water (400 μL), and acetonitrile (400 μL), the resulting mixture was injected into preparative HPLC (mobile phase: acetonitrile/10 mM ammonium formate 65:35; column: COSMOSIL, $5C_{18}$-MS-II, 10 (i.d.) × 250 mm, 5 μm; flow rate: 6 mL min^{-1}; UV detection: 195 nm; retention time: 15 min). The desired fraction was collected into a flask containing 25% ascorbic acid (200 μL) and the organic solvent was removed under reduced pressure. The desired radiotracer was dissolved in a mixture of polysorbate 80, propylene glycol, and saline (0.1:1:10 v/v/v, 4 mL). The total synthesis time including HPLC purification and radiopharmaceutical formulation for intravenous administration was 28 min. The isolated radioactivity was 4.0 GBq at the end of synthesis and the specific radioactivity was 23 GBq μmol^{-1}. The chemical identity of [^{11}C]Ibuprofen methyl ester was confirmed by co-injection with the authentic sample of Ibuprofen methyl ester on analytical HPLC (mobile phase: acetonitrile/water 70:30; column: COSMOSIL, $5C_{18}$-AR-II, 4.6 (i.d.) × 150 mm, 5 μm; flow rate: 1 mL min^{-1}; UV detection: 210 nm; retention time: 5.3 min). The chemical purity analyzed at 210 nm and the radiochemical purity were greater than 99%.

Radiosynthesis of [^{11}C]Naproxen methyl ester (2): The radiosynthesis method was similar to that of [^{11}C]Ibuprofen methyl ester (**1**). [^{11}C]Naproxen methyl ester was purified by semi-preparative HPLC (mobile phase: acetonitrile/water = 65:35; column: COSMOSIL, $5C_{18}$-MS-II, 20 (i.d.) × 250 mm, 5 μm; flow rate: 10 mL min^{-1}; UV detection: 230 nm; retention time: 16 min). The total synthesis time including HPLC purification and radiopharmaceutical formulation for intravenous administration was 32 min. The isolated radioactivity was 2.5 GBq at the end of synthesis, and the specific radioactivity was 37 GBq μmol^{-1}. The chemical identity of [^{11}C]Naproxen methyl ester was confirmed by co-injection with the authentic sample of Naproxen methyl ester on analytical HPLC (mobile phase: acetonitrile/water 65:35; column: COSMOSIL, $5C_{18}$-MS-II, 4.6 (i.d.) × 150 mm, 5 μm; flow rate: 1 mL min^{-1}; UV detection: 230 nm; retention time: 5.5 min). The chemical purity analyzed at 230 nm and the radiochemical purity were greater than 99%.

Radiosynthesis of [^{11}C]Flurbiprofen methyl ester (3): The radiosynthesis method was similar to that of [^{11}C]Ibuprofen methyl ester (**1**). [^{11}C]Flurbiprofen methyl ester was purified by semi-preparative HPLC (mobile phase: acetonitrile/water 75:25; column: COSMOSIL, $5C_{18}$-MS-II, 20 (i.d.) × 250 mm, 5 μm; flow rate: 10 mL min^{-1}; UV detection: 254 nm; retention time: 15 min). The total synthesis time including HPLC purification and radiopharmaceutical formulation for intravenous administration was 35 min. The isolated radioactivity was 5.8 GBq at the end of synthesis, and the specific radioactivity was 41 GBq μmol^{-1}. The chemical identity of [^{11}C]Flurbiprofen methyl ester was confirmed by co-injection with the authentic sample of Flurbiprofen methyl ester on analytical HPLC (mobile phase: acetonitrile/water 60:40; column: COSMOSIL, $5C_{18}$-AR-II, 4.6 (i.d.) × 100 mm, 5 μm; flow rate: 1 mL min^{-1}; UV detection: 254 nm; retention time: 5.9 min). The chemical purity analyzed at 254 nm and the radiochemical purity were greater than 99%.

Radiosynthesis of [^{11}C]Fenoprofen methyl ester (4): The radiosynthesis method was similar to that of [^{11}C]Ibuprofen methyl ester (**1**). [^{11}C]Fenoprofen methyl ester was purified by semi-preparative HPLC (mobile phase: acetonitrile/water 70:30; column: COSMOSIL, 5C$_{18}$-MS-II, 20 (i.d.)×250 mm, 5 μm; flow rate: 10 mL min^{-1}; UV detection: 206 nm; retention time: 17 min). The total synthesis time including HPLC purification and radiopharmaceutical formulation for intravenous administration was 41 min. The isolated radioactivity was 4.8 GBq at the end of synthesis and the specific radioactivity was 43 GBq μmol^{-1}. The chemical identity of [^{11}C]Fenoprofen methyl ester was confirmed by co-injection with the authentic sample of Fenoprofen methyl ester on analytical HPLC (mobile phase: acetonitrile/water 60:40; column: COSMOSIL, 5C$_{18}$-AR-II, 4.6 (i.d.)×100 mm, 5 μm; flow rate: 1 mL min^{-1}; UV detection: 220 nm; retention time: 5.8 min). The chemical purity analyzed at 220 nm and the radiochemical purity were greater than 99%.

Radiosynthesis of [^{11}C]Ketoprofen methyl ester (5): The radiosynthesis method was similar to that of [^{11}C]Ibuprofen methyl ester (**1**). [^{11}C]Ketprofen methyl ester was purified by semi-preparative HPLC (mobile phase: acetonitrile/water 70:30; column: COSMOSIL, 5C$_{18}$-MS-II, 20 (i.d.)×250 mm, 5 μm; flow rate: 10 mL min^{-1}; UV detection: 254 nm; retention time: 12 min). The total synthesis time including HPLC purification and radiopharmaceutical formulation for intravenous administration was 28 min. The isolated radioactivity was 6.1 GBq at the end of synthesis and the specific radioactivity was 63 GBq μmol^{-1}. The chemical identity of [^{11}C]Ketoprofen methyl ester was confirmed by co-injection with the authentic sample of Fenoprofen methyl ester on analytical HPLC (mobile phase: acetonitrile/water 60:40; column: COSMOSIL, 5C$_{18}$-AR-II, 4.6 (i.d.)×100 mm, 5 μm; flow rate: 1 mL min^{-1}; UV detection: 254 nm; retention time: 5.8 min). The chemical purity analyzed at 254 nm and the radiochemical purity were greater than 99%.

Radiosynthesis of [^{11}C]Loxoprofen methyl ester (6): The radiosynthesis method was similar to that of [^{11}C]Ibuprofen methyl ester (**1**). [^{11}C]Loxoprofen methyl ester was purified by semi-preparative HPLC (mobile phase: acetonitrile/10 mM ammonium formate 50:50; column: COSMOSIL, 5C$_{18}$-MS-II, 10 (i.d.)×250 mm, 5 μm; flow rate: 6 mL min^{-1}; UV detection: 220 nm; retention time: 10 min). The total synthesis time including HPLC purification and radiopharmaceutical formulation for intravenous administration was 36 min. The isolated radioactivity was 2.2 GBq at the end of synthesis, and the specific radioactivity was 28 GBq μmol^{-1}. The chemical identity of [^{11}C]Loxoprofen methyl ester was confirmed by co-injection with the authentic sample of Loxoprofen methyl ester on analytical HPLC (mobile phase: acetonitrile/water 45:55; column: COSMOSIL, 5C$_{18}$-MS-II, 4.6 (i.d.)×150 mm, 5 μm; flow rate: 1 mL min^{-1}; UV detection: 220 nm; retention time: 11.6 min). The chemical purity analyzed at 220 nm and the radiochemical purity were greater than 99%.

Radiosynthesis of [^{11}C]Ibuprofen (7): Sodium hydride (1 mg) was added to a stirred solution of methyl (4-isobutylphenyl)acetate in anhydrous DMF (200 μL) under an Ar atmosphere. [^{11}C]CH_3I was transported by a stream of helium (30 mL min^{-1}) and trapped in the mixture at room temperature for 2 min. A total of 300 μL of 2 M sodium hydroxide was added to the reaction mixture, and then it was heated at 50 °C for 1 min. After addition of a solution of 10% formic acid in acetonitrile (300 μL), the mixture was diluted with 50% acetonitrile in water (300 μL). The given reaction mixture was injected into preparative HPLC (mobile phase: acetonitrile/10 mM sodium phosphate buffer (pH 7.4) 34:66; column: COSMOSIL, 5C$_{18}$-MS-II, 20 (i.d.)×250 mm, 5 μm; flow rate: 10 mL min^{-1}; UV detection: 195 nm; retention time: 16 min). The desired fraction was collected into a flask containing 25% ascorbic acid (200 μL), and the organic solvent was removed under the reduced pressure. The desired radiotracer was dissolved in a mixture of polysorbate 80, propylene glycol, and saline (0.1:1:10 v/v/v, 4 mL). The total synthesis time including HPLC purification and radiopharmaceutical formulation for intravenous administration was 33 min. The isolated radioactivity was 5.0 GBq at the end of synthesis, and the specific radioactivity was 34 GBq μmol^{-1}. The chemical identity of [^{11}C]Ibuprofen was confirmed by co-injection with the authentic sample of Ibuprofen on analytical HPLC (mobile phase: acetonitrile/0.1% phosphoric acid 60:40; column: COSMOSIL, 5C$_{18}$-MS-II, 4.6 (i.d.)×150 mm, 5 μm; flow rate: 1 mL min^{-1}; UV detection: 210 nm; retention time: 5.8 min). The chemical purity analyzed at 210 nm and the radiochemical purity of [^{11}C]Ibuprofen were greater than 99%.

Radiosynthesis of [^{11}C]Naproxen (8): The radiosynthesis method was similar to that of [^{11}C]Ibuprofen (**7**). [^{11}C]Naproxen was purified by semi-preparative HPLC (mobile phase: acetonitrile/10 mM sodium phosphate buffer (pH 7.4) 22:78; column: COSMOSIL, 5C$_{18}$-MS-II, 20 (i.d.)×250 mm, 5 μm; flow rate: 10 mL min^{-1}; UV detection: 200 nm; retention time: 19 min). The total synthesis time including HPLC purification and radiopharmaceutical formulation for intravenous administration was 37 min. The isolated radioactivity was 2.7 GBq at the end of synthesis and the specific radioactivity was 30 GBq μmol^{-1}. The chemical identity of [^{11}C]Naproxen was confirmed by co-injection with the authentic sample of Naproxen on analytical HPLC (mobile phase: acetonitrile/1% phosphoric acid 50:50; column: COSMOSIL, 5C$_{18}$-MS-II, 4.6 (i.d.)×150 mm, 5 μm; flow rate: 1 mL min^{-1}; UV detection: 254 nm; retention time: 5.2 min). The chemical purity analyzed at 254 nm and the radiochemical purity were greater than 99%.

Radiosynthesis of [^{11}C]Flurbiprofen (9): The radiosynthesis method was similar to that of [^{11}C]Ibuprofen (**7**). [^{11}C]Flurbiprofen was purified by semi-preparative HPLC (mobile phase, acetonitrile/10 mM sodium phosphate buffer (pH 7.4) 33:67; column: COSMOSIL, 5C$_{18}$-MS-II, 20 (i.d.)×250 mm, 5 μm; flow rate: 10 mL min^{-1}; UV detection: 254 nm; retention time: 14 min). The total synthesis time including HPLC purification and radiopharmaceutical formulation for intravenous administration was 40 min. The isolated radioactivity was 3.5 GBq at the end of synthesis and the specific radioactivity was 47 GBq μmol^{-1}. The chemical identity of [^{11}C]Flurbiprofen was confirmed by co-injection with the authentic sample of Flurbiprofen on analytical HPLC (mobile phase: acetonitrile/1% phosphoric acid 50:50; column: COSMOSIL, 5C$_{18}$-AR-II, 4.6 (i.d.)×100 mm, 5 μm; flow rate: 1 mL min^{-1}; UV detection: 254 nm; retention time: 6.0 min). The chemical purity analyzed at 254 nm and the radiochemical purity were greater than 99%.

Radiosynthesis of [^{11}C]Fenoprofen (10): The radiosynthesis method was similar to that of [^{11}C]Ibuprofen (**7**). [^{11}C]Fenoprofen was purified by semi-preparative HPLC (mobile phase, acetonitrile/10 mM sodium phosphate buffer (pH 7.4) 20:80; column: COSMOSIL, 5C$_{18}$-MS-II, 20 (i.d.)×250 mm, 5 μm; flow rate: 10 mL min^{-1}; UV detection: 206 nm; retention time: 16 min). The total synthesis time including HPLC purification and radiopharmaceutical formulation for intravenous administration was 40 min. The isolated radioactivity was 6.0 GBq at the end of synthesis and the specific radioactivity was 25 GBq μmol^{-1}. The chemical identity of [^{11}C]Fenoprofen was confirmed by co-injection with the authentic sample of Fenoprofen on analytical HPLC (mobile phase: acetonitrile/0.1% phosphoric acid 45:55; column: COSMOSIL, 5C$_{18}$-AR-II, 4.6 (i.d.)×100 mm, 5 μm; flow rate: 1 mL min^{-1}; UV detection: 220 nm; retention time: 8.4 min). The chemical purity at 220 nm was more than 98% and the radiochemical purity of [^{11}C]Fenoprofen was greater than 99%.

Radiosynthesis of [^{11}C]Ketoprofen (11): The radiosynthesis method was similar to that of [^{11}C]Ibuprofen (**7**). [^{11}C]Ketoprofen was purified by semi-preparative HPLC (mobile phase: acetonitrile/10 mM sodium phosphate buffer (pH 7.4) 30:70; column: COSMOSIL, 5C$_{18}$-MS-II, 20 (i.d.)×250 mm, 5 μm; flow rate: 10 mL min^{-1}; UV detection: 254 nm; retention time: 9.7 min). The total synthesis time including HPLC purification and radiopharmaceutical formulation for intravenous administration was 28 min. The isolated radioactivity was 3.8 GBq at the end of synthesis and the specific radioactivity was 40 GBq μmol^{-1}. The chemical identity of [^{11}C]Ketoprofen was confirmed by co-injection with the authentic sample of Ketoprofen on analytical HPLC (mobile phase: acetonitrile/0.1% phosphoric acid 40:60; column: COSMOSIL, 5C$_{18}$-AR-II, 4.6 (i.d.)×100 mm, 5 μm; flow rate: 1 mL min^{-1}; UV detection: 254 nm; retention time: 6.2 min). The chemical purity at 254 nm and the radiochemical purity were greater than 99%.

Radiosynthesis of [^{11}C]Loxoprofen (12): The radiosynthesis method was similar to that of [^{11}C]Ibuprofen (**7**). [^{11}C]Loxoprofen was purified by semi-preparative HPLC (mobile phase: acetonitrile/10 mM sodium phosphate buffer (pH 7.4) 20:80; column: COSMOSIL, 5C$_{18}$-MS-II, 20 (i.d.)×

250 mm, 5 μm; flow rate: 10 mL min^{-1}; UV detection: 220 nm; retention time: 16 min). The total synthesis time including HPLC purification and radiopharmaceutical formulation for intravenous administration was 42 min. The isolated radioactivity was 2.0 GBq at the end of synthesis and the specific radioactivity was 28 GBq μmol^{-1}. The chemical identity of [^{11}C]Loxoprofen was confirmed by co-injection with the authentic sample of Loxoprofen on analytical HPLC (mobile phase: acetonitrile/0.1% phosphoric acid 60:40; column: COSMOSIL, 5C$_{18}$-AR-II, 4.6 (i.d.)×100 mm, 5 μm; flow rate: 1 mL min^{-1}; UV detection: 220 nm; retention time: 6.6 min). The chemical purity at 220 nm and the radiochemical purity were greater than 99%.

Experimental animals: The animals were kept in a temperature- and light-controlled environment and had ad libitum access to standard food and tap water. All experimental protocols were approved by the Ethics Committee on Animal Care and Use of the Center for Molecular Imaging Science in RIKEN, and were performed in accordance with the Principles of Laboratory Animal Care (NIH publication no. 85–23, revised 1985).

Generation of neuroinflammation in rats: Male Sprague-Dawley rats (CLEA Japan, Tokyo, Japan) that weighed approximately 300 g received an injection of lipopolysaccharides (LPS) from *Escherichia coli* 026:B6 (Sigma, St. Louis, MO, USA) into the left striatum. Briefly, animals were anesthetized with 50 mg kg^{-1} sodium pentobarbital and stereotaxically injected with LPS into the left striatum with a Hamilton syringe (anterior: +0.2, lateral: +3.2, ventral: −5.5 mm from bregma). Animals were returned to their home cages after the surgery and were housed for 1 day following LPS injection.

PET studies: Rats were anesthetized with a mixture of 1.5% isoflurane and nitrous oxide/oxygen (7:3) and then placed on the PET scanner gantry (microPET Focus 220, Siemens Co., Knoxville, TN, USA). The PET scanner has a spatial resolution of 1.4 mm in FWHM at the center of the field of view at 220 mm in diameter and an axial extent at 78 mm in length. After intravenous bolus injection of 2-aryl[^{11}C]propionic acid or 2-aryl[^{11}C]propionic acid methyl ester (ca. 70 MBq per animal) by means of a venous catheter inserted into the tail vein, a 45 min emission scan was performed. In the blocking experiment, unlabeled compound (10 mg kg^{-1}) was simultaneously injected with radiotracers. Emission data were acquired in list mode, and the data were reconstructed with standard 2D filtered back projection (Ramp filter, cutoff frequency at 0.5 cycles per pixel). Regions of interest (ROI) were placed on the LPS-injected side and the contralateral side of striatum by using image processing software (Pmod ver.3.0, PMOD Technologies Ltd, Zurich, Switzerland) with reference to the rat MRI. Regional uptake of radioactivity in the brain was decay-corrected to the injection time and expressed as the standardized uptake value (SUV), normalized for injected radioactivity and body weight.

Ex vivo autoradiography: Fifty minutes after tracer injection, rats were euthanized and were perfused with saline under deep anesthesia with 1.5% isoflurane. Their brains were quickly removed, and 2 mm thick coronal sections were prepared by using a brain matrix (RBM-2000C, ASI Instruments, Warren, MI, USA) at 4°C. These brain sections were then placed in contact with imaging plates (BAS SR-2040; FUJIFILM, Tokyo, Japan) for 1 h. Autoradiograms were obtained and quantified by using a Bio-Imaging Analyzer System (FLA7000; FUJIFILM). Radioactivity levels in the brain regions were measured and expressed as photostimulated luminescence (PSL)/area [mm^2].

Radioactive metabolite analysis in brain and blood after administration of [^{11}C]5 to normal rats: Male Sprague-Dawley rats weighing around 200 g (n=9) were anesthetized with 1.5% isoflurane before administration of the radiotracers. After intravenous injection of [^{11}C]**5** (ca. 110 MBq per animal) into the rats, blood sampling was performed, and the blood flow was terminated by transection of the abdominal aorta and vein after 2, 5, and 10 min. The brain was removed quickly and subsequently frozen in liquid nitrogen, and then the mixture was homogenized. Two-fold volumes of acetonitrile were added to blood or brain homogenate aliquot, and then the resulting mixture was centrifuged at 12,000 rpm for 2 min at 4°C. The supernatant was evaporated, reconstituted with HPLC mobile phase, and then analyzed for radioactive components by using an HPLC system (Shimadzu Corporation, Kyoto, Japan) with a coupled NaI(Tl) positron detector UG-SCA30 (Universal Giken, Kanagawa, Japan) to measure intact radiotracer and its acid form. A fast-gradient condition created with two switching pumps was used to analyze the samples. An Atlantis T3 column (4.6 (i.d.)×50 mm; Waters, Milford, MA, USA) was used as a reverse-phase analytical column, and a flow rate of 2.0 mL min^{-1} of methanol/water (28:72, v/v) containing 10 mM ammonium acetate (pH 7.2) was the initial condition used. After 0.3 min of the sample injection, the ratio of acetonitrile/water was changed to 80:20 (v/v) linearly for 2.2 min and maintained for the next 2.0 min. The columns were then washed with acetonitrile/water (28:72, v/v) containing 10 mM ammonium acetate (pH 7.2). The elution was monitored by UV absorbance at 254 nm and coupled NaI positron detection. The amount of radioactivity associated with intact radiotracer and its acid form was calculated as a percentage of the total amount of radioactivity.

Acknowledgements

This work was supported in part by a consignment expense for the Molecular Imaging Program on "Research Base for Exploring New Drugs" from the Ministry of Education, Culture, Sports, Science and Technology (MEXT) of Japan. We would like to thank Mr. M. Kurahashi (Sumitomo Heavy Industry Accelerator Service Ltd.) for operating the cyclotron, Ms. K. Tokuda (RIKEN) for supporting rat PET studies, Ms. E. Hayashinaka (RIKEN) for supporting the reconstruction of PET images, and Dr. M. Murai, Mr. K. Noutomi, and Ms.Y. Katayama (RIKEN) for supporting the metabolite analyses.

[1] J. G. Lombardino, *Nonsteroidal Antiinflammatory Drugs*, Wiley, New York, **1985**.

[2] N. V. Chandrasekharan, H. Dai, K. L. T. Roos, N. K. Evanson, J. Tomsik, T. S. Elton, D. L. Simmons, *Proc. Natl. Acad. Sci. USA* **2002**, *99*, 13926–13931.

[3] a) M. E. Phelps *PET: Molecular Imaging and its Biological Applications*, Springer, New York, **2004**; b) J. S. Fowler, A. P. Wolf, *Acc. Chem. Res.* **1997**, *30*, 181–188; c) S. M. Ametamey, *Chem. Rev.* **2008**, *108*, 1501–1516; d) P. W. Miller, N. J. Long, R. Vilar, A. D. Gee, *Angew. Chem.* **2008**, *120*, 9136–9172; *Angew. Chem. Int. Ed.* **2008**, *47*, 8998–9033.

[4] G. Lappin, R. C. Garner, *Nat. Rev. Drug Discovery* **2003**, *2*, 233–240.

[5] M. Bergström, R. J. Hargreaves, H. D. Burns, M. R. Goldberg, D. Sciberras, S. A. Reins, K. J. Petty, M. Ögren, G. Antoni, B. Långström, O. Eskola, M. Scheinin, O. Solin, A. K. Majumdar, M. L. Constanzer, W. P. Battisti, T. E. Bradstreet, C. Gargano, J. Hietala, *Biol. Psychiatry* **2004**, *55*, 1007–1012.

[6] a) M. Suzuki, K. Sumi, H. Koyama, Siqin, T. Hosoya, M. Takashima-Hirano, H. Doi, *Chem. Eur. J.* **2009**, *15*, 12489–12495; b) H. Doi, I. Ban, A. Nonomiya, K. Sumi, C. Kuang, T. Hosoya, H. Tsukada, M. Suzuki, *Chem. Eur. J.* **2009**, *15*, 4165–4171; c) M. Suzuki, H. Doi, M. Björkman, Y. Andersson, B. Långström, Y. Watanabe, R. Noyori, *Chem. Eur. J.* **1997**, *3*, 2039–2042.

[7] a) H. R. Herschman, J. J. Talley, R. DuBois, *Mol. Imaging. Biol.* **2003**, *5*, 286–303; b) E. F. de Vries, *Curr. Pharm. Des.* **2006**, *12*, 3847–3856; c) S. T. Elder, *Diss. Abstr. Int. B* **1991**, *52*, 2566.

[8] E. F. de Vries, A. van Waarde, A. R. Buursma, W. Vaalburg, *J. Nucl. Med.* **2003**, *44*, 1700–1706.

[9] J. Prabhakaran, V. J. Majo, N. R. Simpson, R. L. Van Heertum, J. J. Mann, J. S. D. Kumar, *J. Labelled Compd. Radiopharm.* **2005**, *48*, 887–895.

[10] E. F. de Vries, J. Doorduin, R. A. Dierckx, A. van Waarde, *Nucl. Med. Biol.* **2008**, *35*, 35–42.

[11] V. J. Majo, J. Prabhakaran, N. R. Simpson, R. L. Van Heertum, J. J. Mann, J. S. D. Kumar, *Bioorg. Med. Chem. Lett.* **2005**, *15*, 4268–4271.

[12] M. Tanaka, Y. Fujisaki, K. Kawamura, K. Ishiwata, Qinggeletu, F. Yamamoto, T. Mukai, M. Maeda, *Biol. Pharm. Bull.* **2006**, *29*, 2087–2094.

[13] a) T. J. McCarthy, A. U. Sheriff, M. J. Graneto, J. J. Talley, M. J. Welch, *J. Nucl. Med.* **2002**, *43*, 117–124; b) Y. Fujisaki, K. Kawamura, W. F. Wang, K. Ishiwata, F. Yamamoto, T. Kuwano, M. Ono, M. Maeda, *Ann. Nucl. Med.* **2005**, *19*, 617–625; c) F. R. Wüst, A. Hohne, P. Metz, *Org. Biomol. Chem.* **2005**, *3*, 503–507; d) J. Prabhakaran, M. F. Underwood, R. V. Parsey, V. Arango, V. J. Majo, N. R. Simpson, R. Van Heertum, J. J. Mann, J. S. D. Kumar, *Bioorg. Med. Chem.* **2007**, *15*, 1802–1807; e) F. Wuest, T. Kniess, R. Bergmann, J. Pietzsch, *Bioorg. Med. Chem.* **2008**, *16*, 7662–7670.

[14] a) J. E. Dinchuk, B. D. Car, R. J. Focht, J. J. Johnston, B. D. Jaffee, M. B. Covington, N. R. Contel, V. M. Eng, R. J. Collins, P. M. Czerniak, S. A. Gorry, J. M. Trzaskos, *Nature* **1995**, *378*, 406–409; b) R. Langenbach, C. Loftin, C. Lee, H. Tiano, *Biochem. Pharmacol.* **1999**, *58*, 1237–1246; c) R. Langenbach, S. G. Morham, H. F. Tiano, C. D. Loftin, B. I. Ghanayem, P. C. Chulada, J. F. Mahler, C. A. Lee, E. H. Goulding, K. D. Kluckman, H. S. Kim, O. Smithies, *Cell* **1995**, *83*, 483–492; d) S. G. Morham, R. Langenbach, C. D. Loftin, H. F. Tiano, N. Vouloumanos, J. C. Jennette, J. F. Mahler, K. D. Kluckman, A. Ledford, C. A. Lee, O. Smithies, *Cell* **1995**, *83*, 473–482; e) J. L. Wallace, A. Bak, W. McKnight, S. Asfaha, K. A. Sharkey, W. K. MacNaughton, *Gastroenterology* **1998**, *115*, 101–109.

[15] M. Takashima-Hirano, Y. Cui, T. Takashima, E. Hayashinaka, Y. Wada, Y. Watanabe, H. Doi, M. Suzuki, *J. Labelled Compd. Radiopharm.* **2009**, *52*, S435.

[16] Although the method by using malonic esters as the precursor for the synthesis of 2-[^{11}C][14]methyl-fatty acids was reported, it requires three steps including methylation, hydrolysis, and decarboxylation to give our desired compounds. See reference: K. Ogawa, M. Sasaki, T. Nozaki, *Appl. Radiat. Isot.* **1997**, *48*, 623–630.

[17] a) T. D. Warner, F. Giuliano, I. Vojnovic, A. Bukasa, J. A. Mitchell, J. R. Vane, *Proc. Natl. Acad. Sci. USA* **1999**, *96*, 7563–7568; b) D. Riendeau, M. Salem, A. Styhler, M. Ouellet, J. A. Mancini, C. S. Li, *Bioorg. Med. Chem. Lett.* **2004**, *14*, 1201–1203.

[18] a) H. Fujisawa, T. Fujiwara, Y. Takeuchi, K. Omata, *Chem. Pharm. Bull.* **2005**, *53*, 524–528; b) T. Bruzzese, M. Cambieri, R. Ferrari, Ger. Offen. DE2614306, **1976**; c) J. H. Fried, I. T. Harrison, S. African ZA6707597, **1968**; d) S. S. Adams, J. Bernard, J. S. Nichlolson, A. R. Blancafort, U.S. Patent 3755427, **1973**; e) Y. L. Chen, U.S. Patent 2005032859, **2005**; f) D. E. Bays, R. V. Foster, S.African ZA6804682, **1969**; g) A. Terada, E. Misaka, K. Hasegawa, Fr. Demande FR2483918, **1981**.

[19] a) T. Fukumura, R. Y. Nakao, M. Yamaguchi, K. Suzuki, *Appl. Radiat. Isot.* **2004**, *61*, 1279–1287; b) P. J. H. Scott, B. G. Hockley, H. F. Kung, R. Machanda, W. Zhang, M. R. Kilbourn, *Appl. Radiat. Isot.* **2009**, *67*, 88–94.

[20] All products were isolated as a racemic mixture. Generally, the *S* enantiomer of 2-arylproiponic acid is pharmacologically active in terms of the cyclooxygenase inhibition. However, the majority of 2-arylpropionic acids are prepared in a racemic mixture because an isomerase enzyme (2-arylpropionyl-CoA epimerase) exists in vivo system that converts the inactive *R* enantiomer into the active *S* form, see: a) C. Reichel, R. Brugger, H. Bang, G. Geisslinger, K. Brune, *Mol. Pharmacol.* **1997**, *51*, 576–582; exceptionally, a few inhibitors, such as Flurbiprofen, undergo such a bioconversion to a very little extent in vitro or in vivo systems, see: b) D. D. Leipold, D. Kantoci, E. D. Murray, D. D. Quiggle, W. J. Wechter, *Chirality* **2004**, *16*, 379–387; optical resolution by chiral column chromatography would be effective to separate racemic-2-aryl[^{11}C]propionic acids and esters into the corresponding *R* and *S* enantiomers, respectively, as exemplified by (*R*)-Flurbiprofen (retention time: 10 min) and (*S*)-Flurbiprofen (retention time: 13 min) (mobile phase: 0.05% trifluoroacetic acid in hexane/0.05% trifluoroacetic acid in ethanol 95:5; column: CHIRALPAK AD-H 10 (i.d.) × 250 mm, 5 μm (Daicel Chemical Industries, Tokyo, Japan); flow rate: 6 mL min^{-1}; UV detection: 254 nm). If necessary, the use of an optically active PET tracer will be reported with the detailed resolution method in due course.

[21] H. B. Choi, J. K. Ryu, S. U. Kim, J. G. McLarnon, *J. Neurosci.* **2007**, *27*, 4957–4968.

[22] J. L. Eriksen, S. A. Sagi, T. E. Smith, S. Weggen, P. Das, D. C. McLendon, V. V. Ozols, K. W. Jessing, K. H. Zavitz, E. H. Koo, T. E. Golde, *J. Clin. Invest.* **2003**, *112*, 440–449.

[23] a) O. Inoue, R. Hosoi, S. Momosaki, K. Yamamoto, M. Amitani, M. Yamaguchi, A. Gee, *Nucl. Med. Biol.* **2006**, *33*, 985–989; b) S. Momosaki, R. Hosoi, T. Sanuki, K. Todoroki, M. Yamaguchi, A. Gee, O. Inoue, *Nucl. Med. Biol.* **2007**, *34*, 939–944.

[24] V. W. Pike, *Trends Pharmacol. Sci.* **2009**, *30*, 431–440.

[25] It should be added that this rapid methylation could also be applied to other 2-arylpropionic acid derivatives of NSAIDs, such as, Benoxaprofen, Cycloprofen, Pranoprofen, etc. to form a larger PET tracer library.

[26] B. Långström, G. Antoni, P. Gullberg, C. Halldin, P. Malmborg, K. Nagren, A. Rimland, H. Svard, *J. Nucl. Med.* **1987**, *28*, 1037–1040.

Received: November 5, 2009
Revised: February 4, 2010
Published online: March 10, 2010

